

PAPER • OPEN ACCESS

Harmonic elimination and dc-link voltage balancing in bipolar hybrid microgrid using Space vector modulation for Interlinking Converter (ILC)

To cite this article: S Vasantharaj and V Indra Gandhi 2020 *IOP Conf. Ser.: Mater. Sci. Eng.* **906** 012021

View the [article online](#) for updates and enhancements.



ECS **240th ECS Meeting**
Oct 10-14, 2021, Orlando, Florida

**Register early and save
up to 20% on registration costs**

Early registration deadline Sep 13

REGISTER NOW

Harmonic elimination and dc-link voltage balancing in bipolar hybrid microgrid using Space vector modulation for Interlinking Converter (ILC)

S Vasantharaj^{1*}, V Indra Gandhi²

¹Research Scholar, Vellore Institute of Technology, Vellore

²Associate Professor, Vellore Institute of Technology, Vellore

*Corresponding author E-mail: Vasantharaj.s@vit.ac.in

Abstract: The modernization of distribution grids developed the power systems towards the smart grid. The microgrid plays a vital role in an improving power systems area, which refers to the loads operated under an organized and synchronized way and the distributed energy resources. The microgrid, which is operated in “islanded” mode, should be connected to the main power grid, or it must be entirely off-grid. Bipolar hybrid microgrid feeds local loads with local resources because it consists of both DC and AC bus simultaneously. The converter, which is used for microgrid application, plays an important role, which is said to be Interlinking Converter (ILC). The lower order harmonics can be eliminated by these ILCs. By reducing the THD and increasing the dc-link voltage utilization SVM is used. In this paper, there will be an increase in system performance and great reliability with a fully automated system. There will be a decrease in switching losses, current ripple and THD of grid current by the use of a new switching modulation method, which is validated by the Matlab simulation results.

Keywords:

Interlinking Converter, THD, dc-link, carrier based modulation, voltage ripple, grid and hybrid microgrid.

Nomenclature:

| | | | |
|-----------|-------------------------------------|-----------|--------------------------|
| ILC | Interlinking Converter | NPC | Neutral Point Clamped |
| SVM | Space Vector Modulation | V_{dcl} | DC-link Voltage |
| DC | Direct Current | VSC | Voltage Source Converter |
| AC | Alternating Current | BHM | Bipolar Hybrid Microgrid |
| U_{ref} | Normalized Reference Voltage Vector | | |
| MG | Microgrid | V_{dc} | DC voltage |
| MLC | Multilevel converter | | |

1. Introduction:

The ILC performs the bidirectional flow of power without any power conversion circuit between dc and ac buses. The distributed power is transferred between utility grids to MG and vice versa [1–3] will be managed by ILCs, which are the essential device of microgrid [4–6]. The proper bidirectional ILC should be selected for the load management and the resources that are connected to the microgrid. The BHM consists of two self-governing AC and DC buses [7]. ILC can control variables of ac or dc bus that act as an interface between the buses. Hence, in an AC microgrid the operation of ILC has two conditions: (1) DC Grid Feeding and AC Grid Forming, (2) AC Grid Feeding and DC Grid Forming [8–11]. The performance of ILC will not be affected by the changes in ac bus but the dc bus voltage will be formed by the ILC. In hybrid microgrid, two level VSC act as a suitable ILC topology for BHM [12]. The proposed work contains more efficiency compared to multilevel ILCs. In various cases by having, more number of voltage levels in dc bus we can able to connected different voltage levels of loads and resources. A boost converter has to be applied to link PV sources to the dc bus, though, when lower dc-link is in range, avoids additional boosting voltage, cost of the converter and volume by joining the PV



to this lower V_{dc} [13]. Alternatively, the voltage balancing challenge will be raised by various V_{dc} levels, which is offered by multilevel converters as ILC.

During high switching frequencies MLC does not accomplish well due to switching power losses. It is well known that in medium and high power applications, multilevel converter needs extra semiconductors [14]. The 10-switch converter performs more advantages in both two level and three level converters that negotiates amongst two level VSCs and MLCs. In [15], it explains about the different types of MLCs, having combination of three-level NPC and two level VSC. In preceding works on 10-switch converter, V_{dcl} balancing problems are not discussed because it is restricted to SPWM methods [16, 18]. The Z source converter that is connected to 10-switch converter produces output voltage of low quality with unbalanced currents with the use of four-vector SVM method. Furthermore, in the switching sequence of SVM by applying two small voltage vectors there will be an increase in THD and decrease in dc-link voltage utilization.

In this proposed SVM a full scale V_{dcl} balancing approach is designed and simulated. The survey has taken for harmonizing the dc-link poles and the same is evaluated for dc-link balancing strategies with the help of this proposed 10-switch converter. The main features of this 10 switch converter is elaborated in Section 2 and explains about the elimination method for lower order harmonics with the analyses of universal control pattern for a grid-tied ILC. The simulation results of this proposed SVM for BHM under balanced and unbalanced conditions are described in Section 4. Similarly, the current THD, voltage across ILC, dc link voltages and dc voltage ripple will be evaluated [19–21]. By the use of this simulation results the benefits of V_{dcl} balancing and suggested modulation method is evaluated.

2. Diagrammatic Representation and Circuit model of ILC

The BHM contains ILC which is shown in Fig. 1. An ac output voltage of 2/3 level with three-wire bipolar dc topology is proposed by 10 switch converter. The conventional voltage source converter (VSC) added with S1A to S4A switches to obtain this proposed converter. This converter comprises of 3 main legs and an auxiliary leg contains 4 switches having three different forms of switching states (P, O, N). The switching states and their illustration is shown in table 1.

Table 1: switching states of ILC

| Switching State | ON switches | | Terminal voltage |
|-----------------|-------------|----------------|------------------|
| P | S1A | S1 or S3 or S5 | E |
| O | S2A | S1 or S3 or S5 | 0 |
| | S3A | S2 or S4 or S6 | |
| N | S4A | S2 or S4 or S6 | -E |

The auxiliary leg of switches S2A or S3A produces a switching state O and these switches depend on former leg states. The remaining switching states are said to be understandable. eight and twenty seven switching vectors of two-level and three-level VSI is compared with the 10-switch converter which has twenty one switching vectors that contains eighteen active and three zero vectors (PPP, OOO, NNN). The twenty-one switching vectors of 10 switch converter is splitted as three zero vectors which are sited midpoint of a hexagon including six large and twelve small vectors. The dc-link poles are short-circuited due to this 10-switch converter by having this medium level vectors. The SVM, which is applied for 10-switch converter, consists of six sectors and these sectors are subdivided into small parts having the shapes of trapezoid and triangle. By using this SVM there will be an increase in ac grid THD, switching configuration and NP voltage deviation.

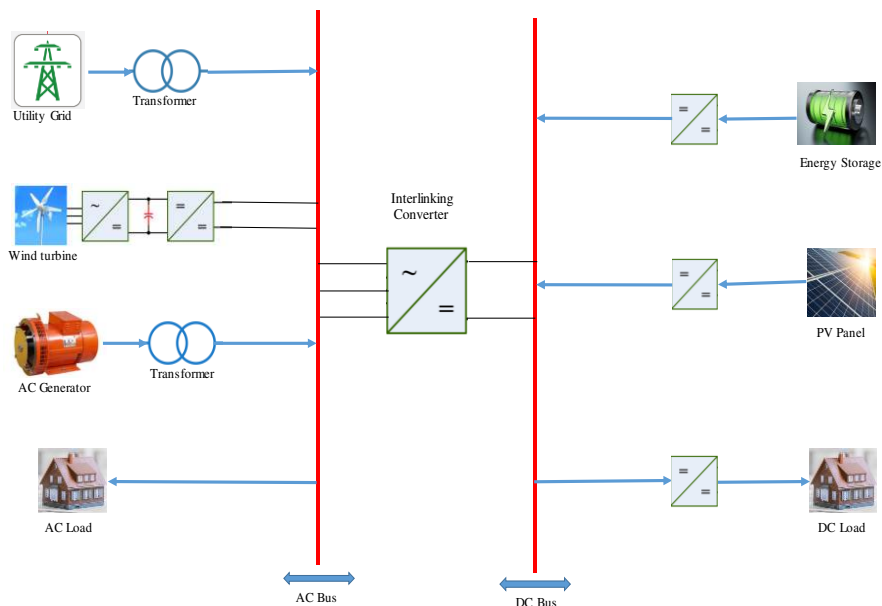


Figure 1. Diagrammatic Representation of Interlinking Converter for Bipolar Hybrid microgrid.

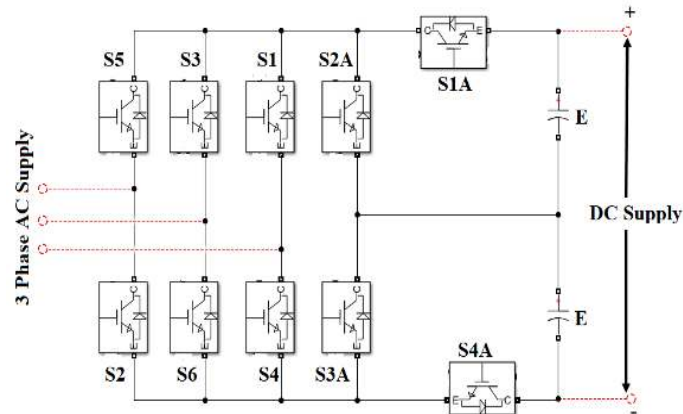


Figure 2. Circuit diagram for ILC.

Fig. 1 shows the bipolar hybrid microgrid with grid tied converter. Similarly, fig 2 represents the circuit diagram of 10 switch interlinking converter. The voltage and frequency on ac bus is controlled by the use of diesel generator, micro turbine or some other converters, that’s why here the ILC is linked to an ac bus. The main purpose of this ILC is to control and stabilize the pole voltages of the DC bus and it is used to inject active and reactive power to ac bus. The THD of ac current in the MG is affected by slight variations in grid, which is produced by the low-order harmonics.

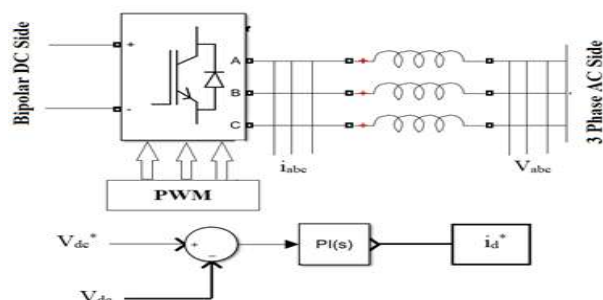


Figure 3. PWM control of ILC.

To overwhelmed these minor distortions effect it consists of two different methods, 1 — feed-forwarding grid voltage [21, 22]. 2 — by interfacing harmonic controller parallel with PI controller. To eliminate lower-order harmonics like fifth and seventh the resonant controller (Gr) is tuned to the same frequency. The basic PWM control of ILC is shown in fig. 3 is upgraded by these usual methods.

$$G_r(s) = \frac{K_r s}{s^2 + (6\omega_n)^2} \tag{1}$$

Where, ω_n is the nominal angular frequency and K_r is the gain.

3. SVM topology and its switching sequence

A V_{dc} balancing ability is elaborated in this subdivision by the use of proposed SVM technique. The main objective of this novel SVM method is to improve dc-link voltage and to decrease the output current THD and common mode voltage. Similarly, this proposed SVM need not have any passive or active elements. The SVM operates under both balanced and unbalanced conditions that lead to decrease in extra converter expenses, volume and loss due to power.

3.1. Region determination

Initially, corresponding SVM for three level VSI, the V_{ref} is induced to measure its angle and amplitude. Then, it is to be determined that were V_{ref} is located and to identify the sector and region for this reference voltage vector. Each sector region is similar to one another and it is validated in fig 4. The region and the sector in which it is situated will be stipulated by the angle and amplitude of the V_{ref} .

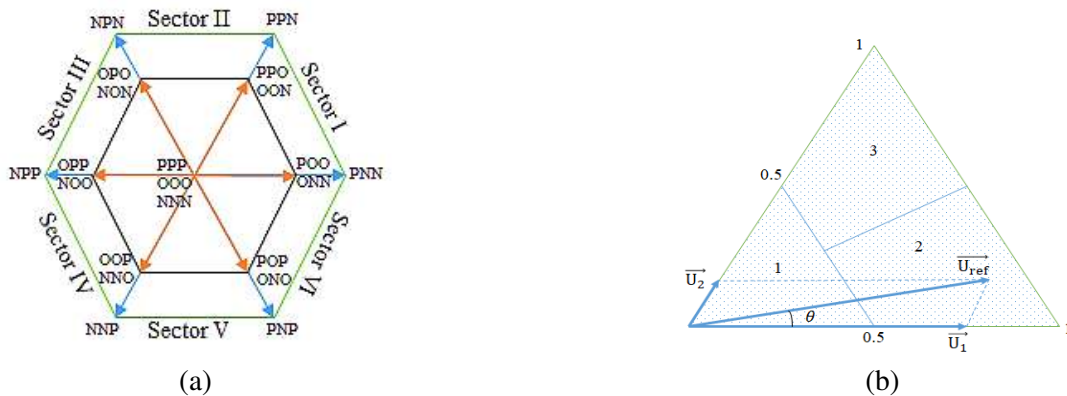


Figure 4. (a) SVM for 10 switch converter (b) Sector representation for normalized voltage vector

The U_{ref} is attained to compute and locate the region of V_{ref} for this 10-switch interlinking converter. The vectors U_1 and U_2 obtain the resultant vector of U_{ref} , which is shown in equation (2), (3) and table 2.

$$U_1 = U_{ref} \left(\cos\theta - \frac{\sin\theta}{\sqrt{3}} \right) \tag{2}$$

$$U_2 = 2U_{ref} \left(\frac{\sin\theta}{\sqrt{3}} \right) \tag{3}$$

To eliminate over modulation these calculations are used. The U_{ref} angle and its amplitude are used to change the region of respective sectors with the values U_1 and U_2 maximum of 1. The U_{ref} amplitude goes in the trapezoidal area, which contains two equal areas after passing region 1 area, which is shown in fig 4. The trapezoidal region changes from 2 to 3 when the reference voltage vector attains 30° which is equal to $\sqrt{3}/2$. The non-existence of medium voltage is reimburse with the split up trapezoidal regions of 2 and 3.

Table 2. Region identification based on U_{ref}

| Case | Angle (θ) | Region |
|--|------------------------|--------|
| $U_1 \leq 0.5$ and $U_2 \leq 0.5$ & $U_1 + U_2 \leq 0.5$ | NA | 1 |
| $U_1 > 0.5$ or $U_2 > 0.5$ or $U_1 + U_2 > 0.5$ | $\theta \leq 30^\circ$ | 2 |
| | $\theta > 30^\circ$ | 3 |

3.2. Symmetrical switching sequence

This type of switching sequence is organized to minimize the THD, which is considered as the main objective of this proposed method.

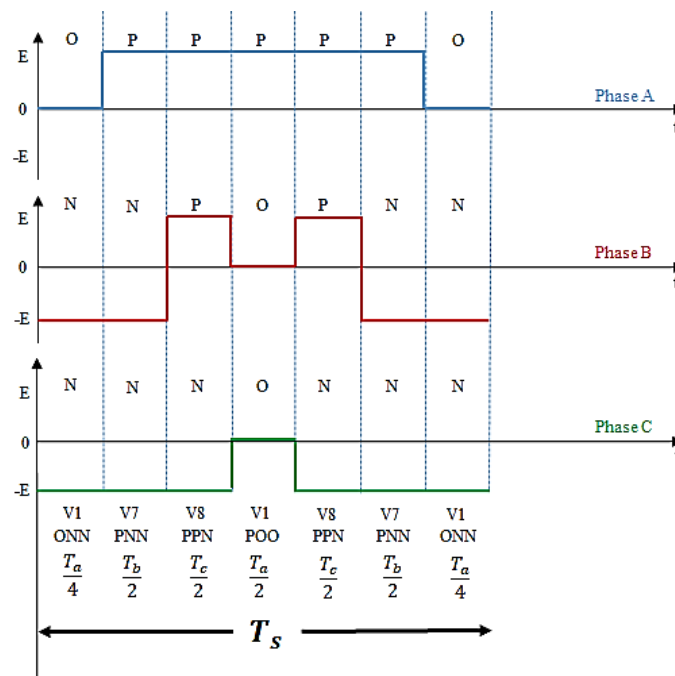


Figure 5. Switching sequence of sector 1.

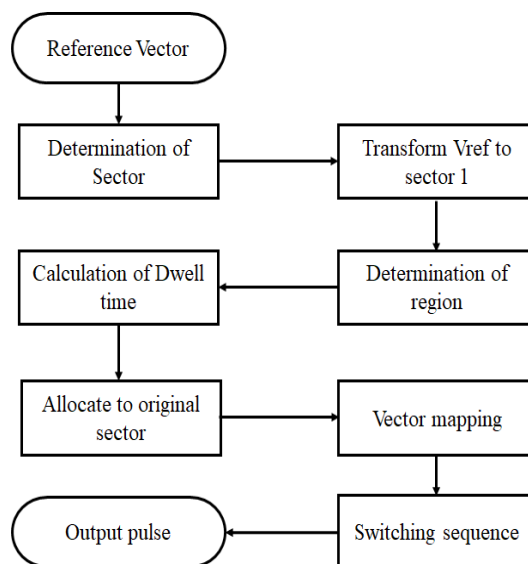


Figure 6. Flowchart for SVM calculation.

The switching time (T_s) for the sector 1 with switching sequence is shown in Fig. 5. Since fig. 4 shows identical sectors and regions, hence by having the reference of first sector, the vector selection and switching sequence of this proposed SVM for all the six sectors eighteen regions are calculated. The selected voltage vectors finalize the switching pattern. Fig. 6 shows the flowchart for the proposed SVM method.

3.3. Voltage balancing with modified switching sequence

In bipolar microgrid, by injecting different and contradictory small voltage vector for 10-switch converter the unbalanced DC-link pole voltage will be rectified. Fig 5 that shows the seven segment switching sequence selects two forms of small vector voltages similarly under balanced condition. Moreover, according to these conditions, it may have five or six segments of switching sequence. For an unbalanced condition, the switching sequence is modified and its states are shown in fig. 7.

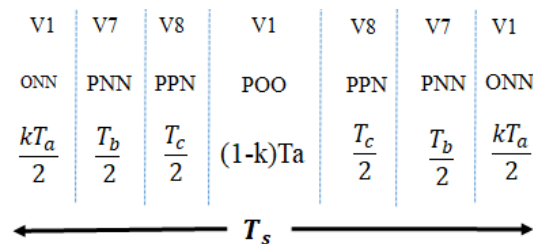


Figure 7. Unbalanced switching Sequence in sector 1.

There will be slow reduction in dc-link pole voltage and escalation in another pole by extracting unequal power from those poles. By using modest and forthright procedure, a coefficient k is determined to find the unbalanced voltages [23]. The interlinking converter that is operated as both rectifier or inverter mode has the value of K regarding the direction of power flow. The 10-switch converter acts as a rectifier mode has the following equations (4) and (5).

$$V_{dc1} - V_{dc2} = V_{Balancing} \tag{4}$$

$$V_{Balancing} > V_{ripple} \Rightarrow K = 1;$$

$$-V_{ripple} \leq V_{Balancing} \leq V_{ripple} \Rightarrow K = 0.5;$$

$$V_{Balancing} < V_{ripple} \Rightarrow K = 0; \tag{5}$$

The dc-link pole voltage ripple is obtained by difference in two dc-link pole voltages and it is denoted as V_{ripple} . The coefficient K becomes 0.5 when the converter works under balanced condition with the absolute value of $V_{balancing}$ is lesser than the V_{ripple} . The coefficient K equals 1 when the converter works under unbalanced condition with the absolute value of $V_{balancing}$ is larger than the V_{ripple} . Hence, by using equations (8) and (9), the coefficient K value can be determined.

4. Simulation Results:

The MATLAB simulated output of the 10 switch-interlinking converter with SVM method for BHM is discussed in this section. The proposed SVM is used to eliminate the harmonics, which is shown, by using FFT spectrum of grid converter output current and voltage. Similarly, controlled dc-link voltage for balanced and unbalanced conditions is examined. Fig 8 shows the MATLAB simulated block diagram for this BHM.

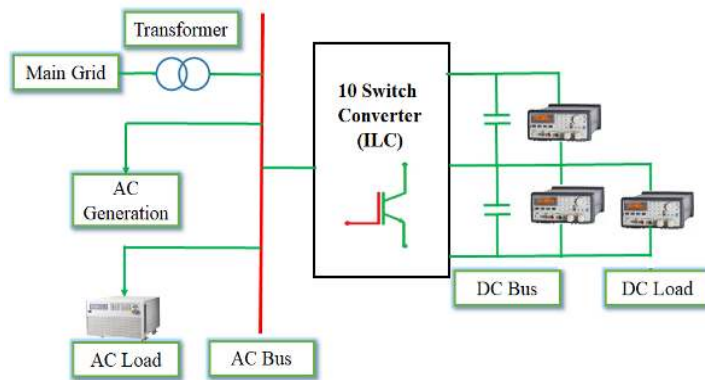


Figure 8. Block Diagram of MATLAB Simulation.

By the use of Matlab Simulink 2014a the ILC with BHM is simulated and the results are discussed below. The Simulink model of MG is simulated under balanced and unbalanced condition for the grid side. Fig. 9 shows the simulated result of PV array and wind energy conversion system.

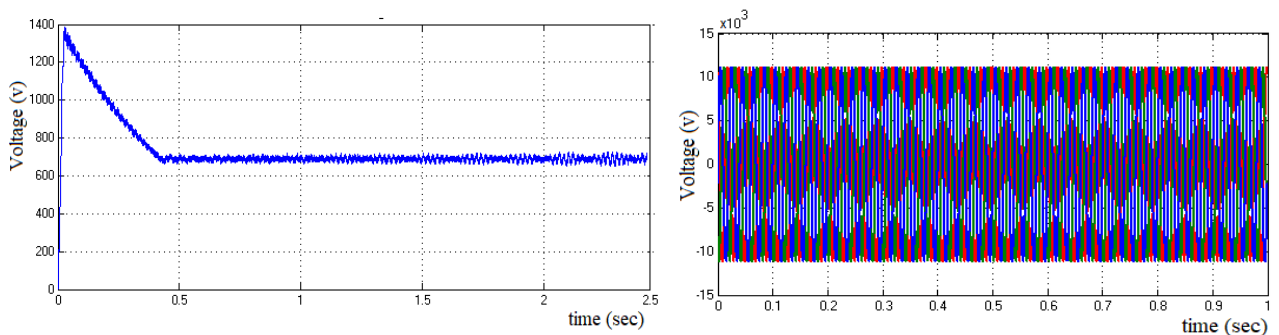


Figure 9. Simulated output of solar PV and Wind energy system

The battery voltage of bipolar hybrid microgrid has a value of 230 V and utility grid that supplies a voltage of 9 kW, which is shown in fig 10. The ac grid under unbalanced condition having a simulated output voltage of 500 V and a current of 5 A which is shown in fig. 11.

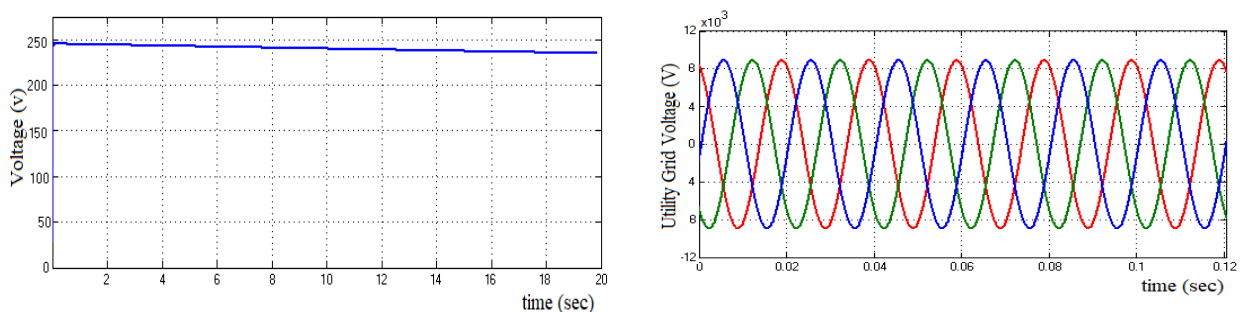


Figure 10. Simulated output of battery and ac utility grid.

The THD analysis for a proposed interlinking converter for an unbalanced condition as a FFT spectrum ac output voltage and current is displayed in fig 12. The output voltage and current has a THD of 20.51% and 12.71%.

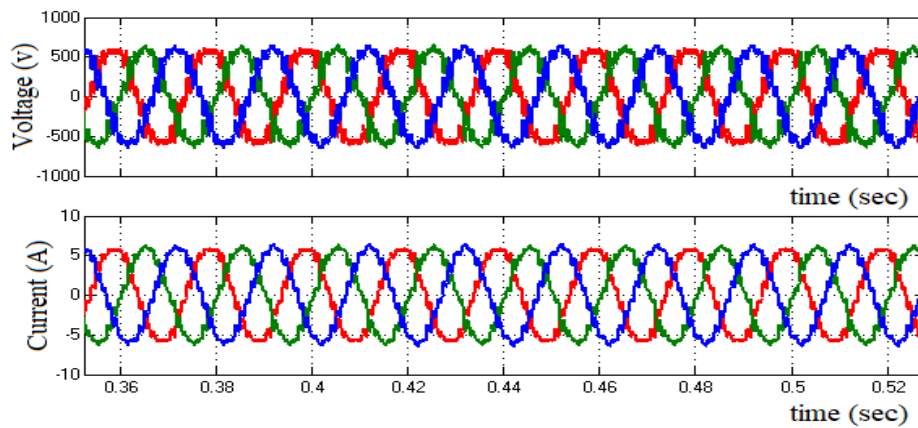


Figure 11. Simulated ac grid side output of Voltage and current for unbalanced condition.

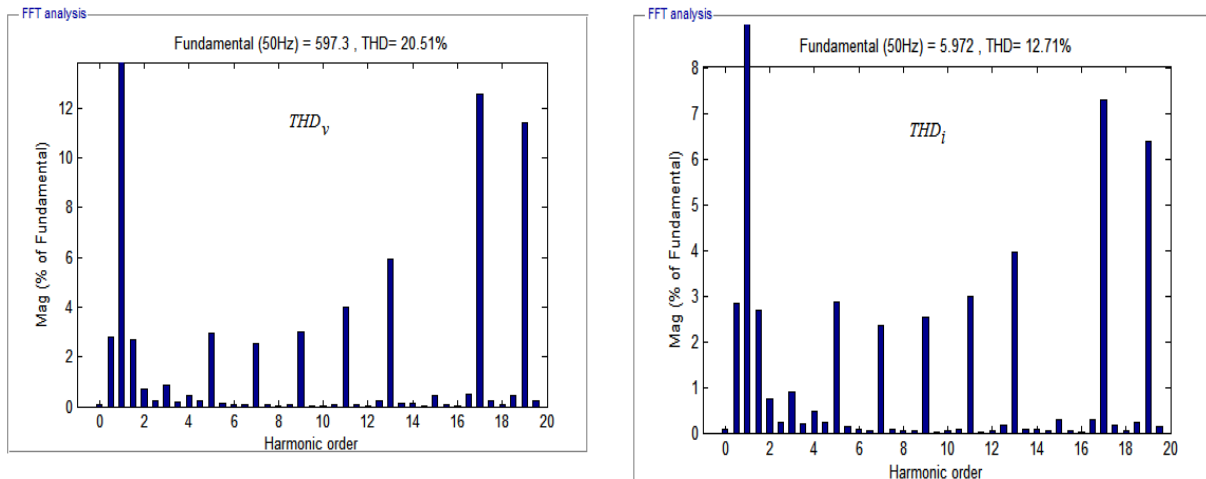


Figure 12. FFT Analysis for grid side output voltage and current for unbalanced condition.

The balanced output voltage and current waveform of grid-connected system is shown in fig. 13. Similarly, fig. 14 shows the balanced condition of grid for this proposed system the THD analysis and FFT spectrum of ac output voltage and current, and their THD are decreased to 12.97% and 4.73%.

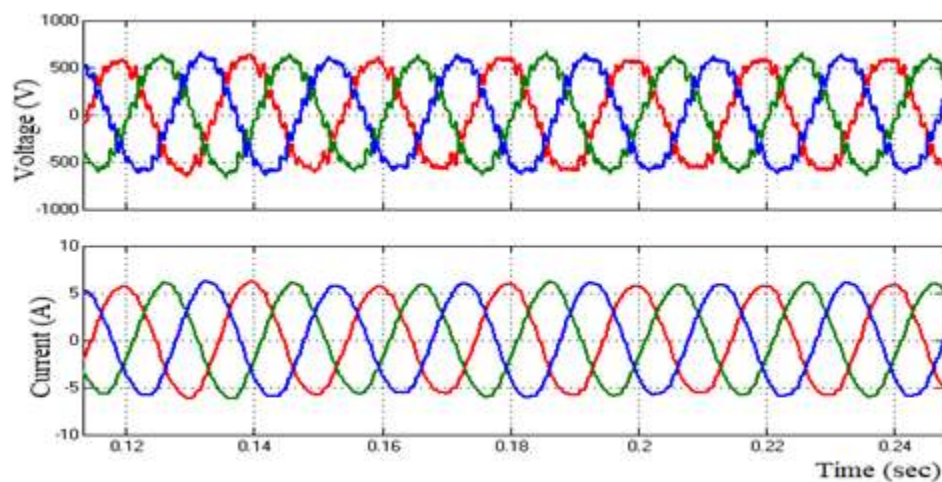


Figure 13. Simulated ac grid side output of Voltage and current for balanced condition.

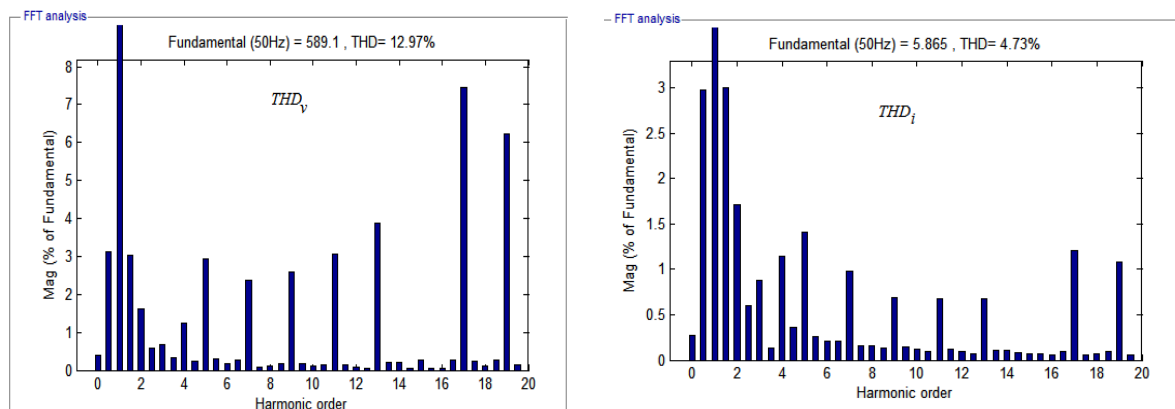


Figure 14. FFT Analysis for grid side output voltage and current for balanced condition.

5. Conclusion:

This paper proposes the working of MG with two-way power flow with the help of ac/dc bidirectional converter and SVM technique. In this proposed SVM method, the grid obtains constant power flow by the use of bidirectional converter under unbalanced condition. This will enrich the consistency of the bidirectional ac/dc converter in weak MG. The efficiency of the MG with bidirectional converter is simulated for balanced and unbalanced grid voltages under dissimilar control schemes. In addition, the renewable energy sources like solar PV and wind energy system features are simulated and the results were discussed. By this proposed SVM technique, the lower order harmonics in the ac grid side are eliminated. The objective of this SVM comprises reduction of current THD in ac grid and increase in V_{del} consumption. Still, the proposed SVM technique is very tough and unites the pole V_{del} in severe unbalance circumstances. The power quality issues and the elimination of lower order harmonics in BHM with 10-switch converter evaluated by the use of proposed SVM is simulated with the help of Matlab Simulink.

Reference:

- [1] Dileep G, A survey on smart grid technologies and applications, *Renewable Energy* 146 (2020) 2589-2625.
- [2] Saurabh Kumar, Vijayakumar K, Simulation and experimental comparative analysis of the DC-DC converter topologies for wind driven SEIG fed DC Nano grid, *Electric Power Systems Research* 181 (2020) 106196.
- [3] Elizabeth Noghreian, Hamid Reza Koofgar, Power Control of hybrid energy systems with renewable sources (wind-photovoltaic) using switched systems strategy, *Sustainable Energy, Grids and Networks* 21 (2020) 100280.
- [4] F. Nejabatkhah, Y.W. Li, Overview of power management strategies of hybrid AC/DC microgrid, *IEEE Trans. Power Electron.* 30 (2015) 7072–7089.
- [5] C. Yin, H. Wu, F. Locment, M. Sechilariu, Energy management of DC microgrid based on photovoltaic combined with diesel generator and super capacitor, *Energy Converters. Manag.* 132 (2017) 14–27.
- [6] E. Hossain, E. Kabalci, R. Bayindir, R. Perez, Microgrid testbeds around the world: State of art, *Energy Converters. Manag.* 86 (2014) 132–153.
- [7] P.C. Loh, D. Li, Y.K. Chai, F. Blaabjerg, Autonomous control of interlinking converter with energy storage in hybrid AC-DC microgrid, *IEEE Trans. Ind. Appl.* 49 (2013) 1374–1382.

- [8] J.Y. Kim, J.H. Jeon, S.K. Kim, C. Cho, J.H. Park, H.M. Kim, K.Y. Nam, Cooperative control strategy of energy storage system and micro sources for stabilizing the microgrid during islanded operation, *IEEE Trans. Power Electron.* 25 (2010) 3037–3048.
- [9] J. Rocabert, G.M.S. Azevedo, A. Luna, J.M. Guerrero, J.I. Candela, P. Rodríguez, Intelligent connection agent for three-phase grid-connected microgrids, *IEEE Trans. Power Electron.* 26 (2011) 2993–3005.
- [10] J. Rocabert, A. Luna, F. Blaabjerg, P. Rodríguez, Control of power converters in AC microgrids, *IEEE Trans. Power Electron.* 27 (2012) 4734–4749.
- [11] X. Lu, J.M. Guerrero, K. Sun, J.C. Vasquez, R. Teodorescu, L. Huang, Hierarchical control of parallel AC-DC converter interfaces for hybrid microgrids, *IEEE Trans. Smart Grid* 5 (2014) 683–692.
- [12] Amir Reza Hassani Ahangar, Gevork B. Gharehpetian, Hamid Reza Baghaee, A review on intentional controlled islanding in smart power systems and generalized framework for ICI in microgrids, *Electrical Power and Energy Systems* 118 (2020) 105709.
- [13] Mohsen Eskandari, Li Li, Mohammad. H. Moradi, Improving power sharing in islanded networked microgrids using fuzzy-based consensus control, *Sustainable Energy, Grids and Networks* 16 (2018) 259–269.
- [14] H. Abu-Rub, J. Holtz, J. Rodriguez, G. Baoming, Medium-voltage multilevel converters State of the art, challenges, and requirements in Industrial applications, *IEEE Trans. Ind. Electron.* 57 (2010) 2581–2596.
- [15] R. Rahimi, G.R. Moradi, E. Afshari, B. Farhangi, S. Farhangi, Study of leakage current phenomena in hybrid 2/3-level three-phase transformerless photovoltaic grid-connected inverters, in: 1st Int. Conf. New Res. Achiev. Electr. Comput. Eng., 2016.
- [16] Hammad Armghan, Ming Yang, Ammar Armghan, Naghmash Ali, M. Q. Wang, Iftikhar Ahmad, Design of integral terminal sliding mode controller for the hybrid AC/DC microgrids involving renewables and energy storage systems, *Electrical Power and Energy Systems* 119 (2020) 105857.
- [17] J.H.G. Muniz, E.R.C. Da Silva, R.B. Da Nobrega, E.C. Dos Santos, An improved pulse-width-modulation for the modified hybrid 2/3-level converter, in: 2013 Brazilian Power Electron. Conf. COBEP 2013 - Proc. 2013, pp. 248–253.
- [18] Reza Ghanizadeh, Gevork B. Gharehpetian, Distributed hierarchical control structure for voltage harmonic compensation and harmonic current sharing in isolated microgrids, *Sustainable Energy, Grids and Networks* 16 (2018) 55 – 69.
- [19] Mohamed R. Amer, Osama A. Mahgou, New switching technique for current control of grid converters for wind power systems, *Sustainable Energy, Grids and Networks* 9 (2017) 1–12.
- [20] T. Abeyasekera, C.M. Johnson, D.J. Atkinson, M. Armstrong, Suppression of line voltage related distortion in current controlled grid connected inverters, *IEEE Trans. Power Electron.* 20 (2005) 1393–1401.
- [21] X. Wang, X. Ruan, S. Liu, C.K. Tse, Full feedforward of grid voltage for grid connected inverter with LCL filter to suppress current distortion due to grid voltage harmonics, *IEEE Trans. Power Electron.* 25 (2010) 3119–3127.
- [22] Sunghyok Kim, Songchol Hyon, Chonung Kim, Distributed virtual negative – sequence control for accurate imbalance power sharing in islanded microgrids, *Sustainable Energy, Grids and Networks* 16 (2018) 28 – 36.